Estimation of Absorbed Doses in Humans Due to Intravenous Administration of Fluorine-18-Fluorodeoxyglucose in PET Studies

Alvaro A. Mejia, Takashi Nakamura, Itoh Masatoshi, Jun Hatazawa, Matsumoto Masaki, and Shoichi Watanuki

Division of Radiation Protection and Division of Nuclear Medicine, Cyclotron and Radioisotope Center of Tohoku University, Aramaki-Aoba, Japan

Radiation absorbed doses due to intravenous administration of fluorine-18-fluorodeoxyglucose in positron emission tomography (PET) studies were estimated in normal volunteers. The time-activity curves were obtained for seven human organs (brain, heart, kidney, liver, lung, pancreas, and spleen) by using dynamic PET scans and for bladder content by using a single detector. These time-activity curves were used for the calculation of the cumulative activity in these organs. Absorbed doses were calculated by the MIRD method using the absorbed dose per unit of cumulated activity, "S" value, transformed for the Japanese physique and the organ masses of the Japanese reference man. The bladder wall and the heart were the organs receiving higher doses of 1.2×10^{-1} and 4.5×10^{-2} mGy/MBq, respectively. The brain received a dose of 2.9×10^{-2} mGy/MBq, and other organs received doses between 1.0×10^{-2} and 3.0×10^{-2} mGy/MBq. The effective dose equivalent was estimated to be 2.4×10^{-2} mSv/MBq. These results were comparable to values of absorbed doses reported by other authors on the radiation dosimetry of this radiopharmaceutical.

J Nucl Med 1991; 32:699–706

Absorbed doses resulting from nuclear medicine studies are used to compare the benefit of a procedure with its potential risk (*1*). The mean absorbed dose (D) in a target organ (r_k) from a radionuclide distributed uniformly in a source organ (r_h) can be calculated by the MIRD formulation as:

$$D(r_k \leftarrow r_h) = \tilde{A}_h S(r_k \leftarrow r_h), \qquad \text{Eq. 1}$$

where $\tilde{A}$ is the cumulated activity in the source organ and "S" is the absorbed dose per unit of cumulated activity for a particular radionuclide and source-target configuration. "S" values are tabulated for many pairs of organs and radionuclides for the European and American adult reference man by Snyder et al. (*2*), but the biokinetic information which is necessary to estimate the cumulated activity in source organs is scarce in humans and, when available, relates to only a few organs (*3*).

Estimation of absorbed doses due to the intravenous administration of fluorine-18-fluorodeoxyglucose ([^{18}F]FDG) has been reported previously (*4–6*), since this radiopharmaceutical is widely used in conjunction with positron emission tomography (PET) in studies of glucose metabolism in humans. Most of these results are based chiefly on animal biodistribution data of Gallagher et al. (*6*), and only the work of Jones et al. (*7*) presents absorbed doses estimated from measurements in man for the brain and bladder wall. Recently, the ICRP (*3*) also reported the absorbed doses and effective dose equivalent (EDE) resulting from the administration of FDG based on published data (*6–8*).

In this study, we performed measurements of the time-activity curves in six human organs as well as the brain and bladder after the administration of [^{18}F]FDG. Activity measurements were made with PET to define the tissue concentrations of the injected radioactive tracer (*9*). Calculations were carried out by using the MIRD method, with the "S" tables modified for both the Japanese physique (*10*) and the organ masses of the Japanese reference man (*11*) for a more realistic estimation of the absorbed doses.

MATERIALS AND METHODS

Biokinetic data in human were obtained from clinical PET studies with [^{18}F]FDG performed at the Cyclotron and Radioisotope Center (CYRIC) of Tohoku University. Subjects were normal volunteers (a total of 18; age: 23–60) from whom informed consent for measurements of organ metabolism with FDG was obtained. Data obtained before 1987 were included in this study. Measurements for 31 sets of data from seven organs with scarce metabolic data were available for this study. In some instances, data for more than one organ were obtained in the same subject. The number of data per organ and the administered activity to each subject are described in Table 1.

Received Apr. 3, 1990; revision accepted Oct. 11, 1990.

For reprints contact: Prof. Takashi Nakamura, Cyclotron and Radioisotope Center, Tohoku University, Aramaki-Aoba, Sendai 980, Japan.

TABLE 1
Administered Activities and Organs Evaluated in Humans by PET

Subject	Organs	Injected activity (MBq)
1	Pancreas	1.85×10^2
2	Liver and kidney	3.14×10^2
3	Liver and spleen	3.07×10^2
4	Kidney	1.07×10^2
5	Kidney, liver, pancreas, and spleen*	9.62×10^1
6	Kidney, liver, pancreas, and spleen	1.07×10^2
7	Heart and lung	1.85×10^2
8	Heart and lung	2.29×10^2
9	Heart and lung	2.45×10^2
10	Heart and lung	3.70×10^2
11	Heart and lung	9.99×10^1
12	Lung	2.22×10^2
13	Brain	7.40×10^1
14	Brain	2.33×10^2
15	Brain	1.78×10^2
16	Brain*	1.78×10^2
17	Brain*	1.55×10^2
18	Brain	1.33×10^2

Data per organ: brain = 6, heart = 5, kidney = 4, liver = 4, lung = 6, pancreas = 3, and spleen = 3.

* Bladder activity was measured in these subjects up to 2 hr.

Organ Time-Activity Measurements

The amount of injected activity was measured in a dose calibrator and ranged from 74 to 370 MBq (Table 1). Activity measurements in the organs were performed with the ECAT II and PT 931 tomographs built by ORTEC (Oak Ridge, TN) and CTI (Knoxville, TN), respectively. The ECAT II is a single-slice device with spatial resolution of 10.9 and 12.4 mm (FWHM) at the center of the field of view (FOV) using high- and medium-resolution shadow shield, respectively. The PT 931 provides seven images simultaneously and has 8 mm (FWHM) of spatial resolution in the tomographic plain and 10 mm in the axial direction. The tomographs are calibrated periodically before every clinical session to obtain the efficiency of the system. Calibration was performed as described by Hoffman and Phelps (*12*) by measuring a positron-emitting source with the PET system, usually as a uniform solution of activity contained in a cylindrical phantom followed by the measurement of the amount of activity in an aliquot of the solution with a calibrated radiation detector (e.g., well counter). This type of calibration gave the efficiency of the system's response in terms of activity per unit of volume or concentration, which permitted the PET image to be scaled by this calibration factor to be equal to the activity at that location in the subject. Phantom studies showed a percentage of error of 1%–6% for the activity determined by PET, compared to the actual activity measured by the calibrated well counter. Two subjects were also scanned at bladder level and the activity in bladder content (urine) determined by PET showed a difference of 5% with that measured by the well counter.

To obtain quantitative data, proper attenuation correction of the emission data was done by measured or calculated attenuation correction factors. Partial volume effect was minimized using a resolution volume larger than the system's resolution element size. Data were also computer-corrected for deadtime and physical decay.

The time course of the activity was measured by dynamic PET scans often consisting of 5-min sequential scans for a metabolic study of about 1 hr, with the exception of some brain studies for which data were measured up to 2 hr. Regions of interest (ROIs) were set on the organs in the computer-reconstructed image and the average counts per pixel were converted to MBq/g by a cross-calibration factor between the PET system, the well counter, and the dose calibrator. A uniform distribution of activity was assumed, and the total activity in the organ was obtained by multiplying the average activity per gram by organ weight (average organ weight of the Japanese reference man). Data were obtained for the brain, heart, kidney, liver, lung, pancreas, and spleen.

Bladder Time-Activity Measurements

Time-activity curves for bladder content were measured in eight normal volunteers who were well hydrated before the study. Activity was monitored for 1–2 hr with a heavily collimated CsI detector (Kouken-Densi, Co. Ltd., Osaka, Japan) ($1 \times 1 \times 1$ cm^3) and recorded by a multichannel analyzer in the multichannel scale (MCS) mode. The detector and collimator were mounted on a flexible support and placed above the subject's bladder. After the completion of the study, the subject voided and the total activity in urine was determined from a urine sample taken from the total voided volume and measured by the well counter. The activity present in the bladder at 4 hr after injection was also determined in two well-hydrated subjects who voided at 2 hr after injection.

Blood Activity Clearance

Samples of venous blood were taken every 15 sec for 2 min, every 30 sec for 4 min, every 1 or 2 min for 10 min, and every 10 min up to 1 hr and measured in the well counter. These data were used to fit the PET data for the brain and heart according to the three-compartment model for FDG as described later.

Cumulated Activity Calculations

The measured time-activity curves in source organs, corrected for physical decay, were fitted by least squares methods to the function of two exponential terms (Equation A1). For organs with limited biologic disappearance data, the cumulated activity was calculated according to the method suggested by Smith (*13*). In this method, the activity remaining in the organ after the last time measurement is approximated to decrease only by physical decay. The equation used for the calculation of the cumulated activity is described in the Appendix. For the brain and heart, the activity increased with time after injection. Because of the difficulty in predicting the time-course of activity in these organs after the last measurement, the time-activity curves were analyzed by the FDG technique based on the ^{14}C-2-deoxyglucose method developed by Sokoloff et al. (*14*). In this approach, FDG metabolism is represented by a three-compartment model. A complete description is presented in Reference 15. Knowledge of the blood time-activity concentrations is necessary to solve the mathematical model. Kinetic rate constants of the model were determined by a least squares fitting program, SALS (*16*). Physical decay was added to the resulting time-activity functions, expressed in Equation A3, which were later integrated to obtain the cumulated activity in the brain and heart (Equation A4).

Cumulated Activity in the Bladder

The cumulated activity in the bladder was calculated using the procedure described by Jones et al. (*6*). It was determined from the measured bladder time-activity curves (not decay-corrected) and the total activity measured in the bladder at void time, since the cumulated activity, $\tilde{A}$, and the area under the time-activity curve, R, are related to the total activity at void time, A, and the height of the curve at this time, H, by the proportionality:

$$\frac{\tilde{A}}{R(\%\cdot h)} = \frac{A(MBq)}{H(\%)}. \qquad \text{Eq. 2}$$

To account for activity clearance in the bladder after 2 hr, the percent of injected activity in the bladder between 2 and 4 hr was determined in two subjects and the contribution of this additional activity to the bladder wall was included in the absorbed dose calculation.

Cumulated Activities in Other Organs

For the ovaries, organ uptake was estimated from the tissue biodistribution data of Gallagher et al. (*7*) at 1 hr after injection. Organ uptake in the testes and red marrow were estimated from their relative weights to total body (*11*). Instantaneous uptake and an effective half-life of 1.83 hr (physical half-life of ^{18}F) was assumed and the cumulated activity in these organs was calculated as follows:

$$\tilde{A} = 1.443\ A_0 T_{eff}. \qquad \text{Eq. 3}$$

Cumulated activity for the remainder of the body (rb) was obtained as the difference between the cumulated activity in the total body (tb) and the sum of the mean cumulated activity in each source organ (h_i) or

$$\tilde{A}_{rb} = \tilde{A}_{tb} - \sum_i \tilde{A}_{hi}. \qquad \text{Eq. 4}$$

Absorbed Dose Calculations

Absorbed doses to target organs were calculated by the MIRD method. Due to differences in physique between European and American adults and Japanese adults, we used for calculations the MIRD "S" Tables transformed for the Japanese physique by Yamaguchi et al. (*10*) and organ weights of the Japanese adult reference man (*11*). For heart, brain, and red marrow, "S" values were not tabulated. For these organs and the remainder of the body, "S" values were calculated as given in the Appendix.

The mean total absorbed dose to the target organs, D_k, was calculated as

$$D_k = \sum_h [\tilde{A}_h S(r_k \leftarrow r_h)] + \tilde{A}_{rb} S(r_k \leftarrow rb). \qquad \text{Eq. 5}$$

This dose represents the contributions from all the source organs listed in Table 2. For the bladder wall, the contribution from the bladder content was multiplied by a factor of 1.1 that took into account the additional dose due to the activity clearance in the bladder between 2 and 4 hr after injection.

The effective dose equivalent, H_E, as defined by the ICRP 26 (*17*), was obtained by the following equation:

$$H_E = \sum^{k} W_k H_k, \qquad \text{Eq. 6}$$

where w_k is the weighting factor of the organ and H_k is equal to the mean absorbed dose D_k, since the quality factor for ^{18}F is taken as a unit.

Absorbed dose calculations were also performed for European and American adults by using the %ID/g of tissue obtained in this work with the MIRD "S" values of Snyder et al. (*2*) and organ masses of the European and American adult reference man to compare the difference with the results obtained for Japanese adults.

TABLE 2
Organ Uptake of [^{18}F]FDG in Humans*

Organ	Percent of injected activity
Brain	6.9
Heart	3.3
Kidney	1.3
Liver	4.4
Lungs	0.9
Ovary	0.01
Pancreas	0.3
Red marrow	1.7
Spleen	0.4
Testes	0.04
Bladder content	6.3
Remainder of the body	74.4
Total	99.95

* Determined from their cumulated activities with the exceptions of the ovary, which was assumed from dog biodistribution data, and the testes and red marrow, which were estimated from their relative weights.

RESULTS

Time-Activity Curves

Typical time-activity curves measured by PET in seven source organs are shown in Figure 1. As shown in Figure 1, FDG is rapidly incorporated in the brain and heart and also is rapidly cleared from the other organs. Activity is expressed as the percentage of the injected activity per gram of tissue and the lines represent the least squares fitting results that were well fitted to the measured data.

Bladder time-activity curves obtained by a single detector system during 1 or 2 hr are shown in Figure 2. The data were normalized to represent the percentage of injected activity (not decay-corrected), clearing from the bladder after injection. Fluctuations in the data are due to variations in urine excretion. Subject 4 showed a higher excretion of 26.5% of the injected activity at 1 hr void time.

Organ Uptake of [^{18}F]FDG

The percentages of organ uptake of FDG (Table 2) were estimated from their measured activities, except for the ovaries, which were calculated from the dog biodistribution data of Gallagher et al. (*7*); relative weights were used for the testes and red marrow. A 74.4% of uptake for the remainder of the body was obtained, which was close to the value of 70% given by Jones et al. (*6*).

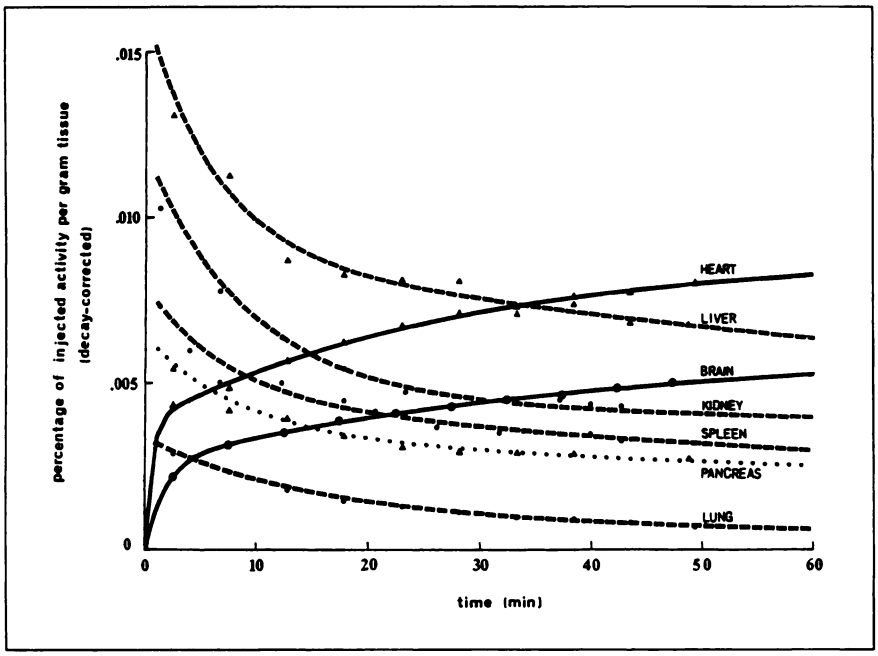

FIGURE 1. Typical time-activity curves measured by PET in seven human organs. The activity is expressed as percent of injected activity per gram of tissue. The lines correspond to the fitting curve adjusted to the measured activity data.

Cumulated Activities

Cumulated activities in source organs calculated by Equation A2 for the kidney, liver, lung, pancreas, and spleen and by Equation A4 for the brain and heart are listed in Table 3. The brain, heart, and liver are the organs showing high cumulated activity. Table 4 shows the cumulated activities calculated by Equation 3 for the ovaries, testes, and red marrow and by Equation 4 for the rest of the body.

Table 5 shows the cumulated activities and percentage of injected activity (decay-corrected to injection time) present in the bladder at 1 or 2 hr void time. Mean percentages of injected activity in the bladder were 19.6% ± 10.9% and 21.2% ± 5.0% at 1 and 2 hr, respectively.

Absorbed Doses

Estimated absorbed doses to target organs per unit of injected activity are summarized in Table 6. Mean values and standard deviations are shown for the contribution from the organ itself (self-dose). The total dose was obtained from Equation 5. The bladder wall received the highest dose. The heart, brain, and kidney also received high absorbed doses of more than 2.7×10^{-2} mGy/MBq.

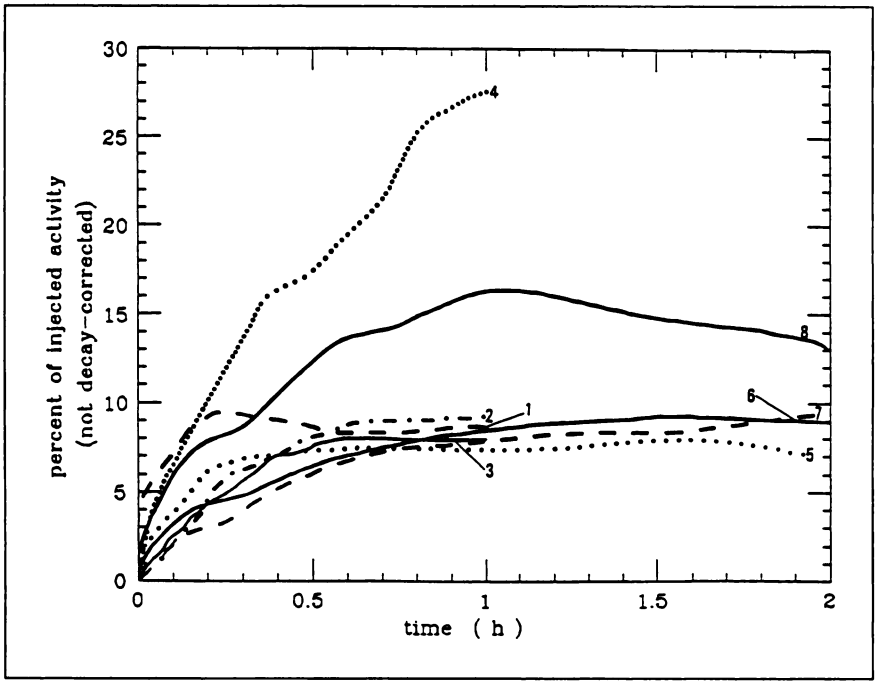

FIGURE 2. This figure shows the smoothed time-activity curves for bladder content obtained in humans 1 or 2 hr after injection of FDG. Data were not decay-corrected, and the numbers in the figure are used to represent the subjects in Table 5.

TABLE 3
Cumulated Activities* per Unit of Administered Activity† in Seven Source Organs

Brain	Heart	Kidneys	Liver	Lungs	Pancreas	Spleen
(MBq·h)						
9.03	4.28	1.50	3.65	0.81	0.25	0.44
7.63	2.47	1.13	3.16	1.05	0.31	0.33
6.65	3.45	1.63	3.76	0.74	0.34	0.38
4.38	2.22	0.79	5.99	0.90		
5.26	3.31			0.79		
6.48				0.85		
Mean ± s.d.						
6.57 ± 1.51	3.15 ± 0.74	1.26 ± 0.33	4.14 ± 1.09	0.86 ± 0.10	0.30 ± 0.04	0.38 ± 0.04

* Determined from measurements in humans.
† Administered activity of 37.0 MBq.

DISCUSSION

The growing importance of FDG as a radiopharmaceutical for metabolic studies makes it necessary to determine the radiation absorbed doses derived from administration of this compound. We calculated the absorbed dose to the brain, lung, heart, kidney, pancreas, spleen, testes, and red marrow based on biokinetic data obtained in humans.

The heart and brain, organs with high hexokinase activity, showed higher activities per gram of tissue (Fig. 1). Similar results were obtained by Jones et al. (*6*).

The mean percentage of injected activity excreted to the bladder at 2 hr void time (21.2%) obtained in this work agreed with the mean value of 20% reported by Jones et al. (*6*). At 1 hr void time, Subject 4 showed a high level of activity in the bladder (38.4%), which is over 2 s.d. of the mean for the other subjects. This subject was included in the absorbed dose estimation to the bladder wall because his study results led to a conservative estimate of the absorbed dose. The variability in bladder activity could be due to differences in the tubular reabsorbtion of ^{18}F-2-FDG (*18*). However, if we exclude the extreme case of Subject 4, a mean value of 13.3% ± 0.9% is obtained that is almost half of that at 2 hr void time. At 4 hr after injection, the activity excreted in the bladder determined in two subjects was 5% and 11% of that obtained at 2 hr with a mean value of 8% that was used in the calculation of the absorbed dose to the bladder wall.

In the calculation of the cumulated activity in some source organs, we have assumed only physical decay of the activity remaining in the organ after the last measurement, since we cannot be certain whether the activity in the organ will disappear at a rate predicted by the fitting results obtained from limited biologic disappearance data. Thus, the calculated cumulated activities in these organs as well as absorbed doses are overestimated because biologic elimination has been neglected.

Absorbed doses estimated in this work were compared to the results reported in other works and are shown in Table 7. Values with double daggers indicate absorbed doses estimated from data in humans, while other results were estimated from animal biodistribution data. Our results concerning the bladder wall agreed with those of Jones et al. in humans (*6*) and also confirmed Jones' theory that the absorbed dose to this organ can be reduced

TABLE 4
Cumulated Activities in Other Source Organs

Organ	Cumulated Activities (MBq·h)
Ovaries*	0.01
Testes†	0.04
Red marrow†	1.62
Remainder of the body‡	72.23

* Estimated from organ biodistribution data in dog at 1 hr (7).
† Estimated from their relative weights.
‡ Calculated as the difference of the cumulated activity in total body minus the sum of the activities in the source organs.

TABLE 5
Cumulated Activities in Bladder Content per Unit of Administered Activity* at One- and Two-Hour Void Time

Subject	Void time (h)	Cumulated activity (MBq·h)	% of injected activity in bladder at void time†
1	1	2.93	12.8
2	1	2.40	14.6
3	1	2.23	12.6
4	1	4.93	38.4
5	2	4.97	14.9
6	2	5.82	18.2
7	2	6.55	24.1
8	2	6.70	27.7
At 1 hr		‡3.12 ± 1.07	‡19.6 ± 10.9
At 2 hr		‡6.01 ± 0.69	‡21.2 ± 5.0

* For injection of 37.0 MBq.
† Decay-corrected to injection time.
‡ Mean ± s.d.

TABLE 6
Absorbed Dose to Various Organs Due to the Intravenous Administration of [^{18}F]FDG

Target organs	Absorbed dose per unit of administered activity (mGy/MBq) Self-Dose*	From bladder content	From remainder of the body	From other source organs	Total dose
Adrenals		8.6×10^{-5}	1.5×10^{-2}	2.6×10^{-3}	1.8×10^{-2}
Bladder wall		* 1.1×10^{-1}	1.0×10^{-2}	1.3×10^{-5}	† 1.2×10^{-1}
		$\pm 1.3 \times 10^{-2}$			‡ 6.6×10^{-2}
Bone surface		7.5×10^{-4}	1.1×10^{-2}	2.9×10^{-3}	1.5×10^{-2}
Brain	$2.9 \times 10^{-2} \pm 6.7 \times 10^{-3}$				2.9×10^{-2}
Breast		5.2×10^{-6}	9.3×10^{-3}	7.5×10^{-4}	1.0×10^{-2}
Stomach wall		1.2×10^{-4}	1.4×10^{-2}	1.4×10^{-3}	1.5×10^{-2}
Small intestine		9.6×10^{-4}	1.5×10^{-2}	7.1×10^{-4}	1.7×10^{-2}
ULI wall		8.7×10^{-4}	1.5×10^{-2}	9.8×10^{-4}	1.7×10^{-2}
LLI wall		2.6×10^{-3}	1.5×10^{-2}	2.0×10^{-4}	1.8×10^{-2}
Heart	$4.5 \times 10^{-2} \pm 1.0 \times 10^{-2}$				4.5×10^{-2}
Kidneys	$2.3 \times 10^{-2} \pm 5.9 \times 10^{-3}$	1.4×10^{-4}	6.1×10^{-3}	1.3×10^{-3}	3.0×10^{-2}
Liver	$1.6 \times 10^{-2} \pm 4.4 \times 10^{-3}$	1.0×10^{-4}	5.7×10^{-3}	5.5×10^{-4}	2.3×10^{-2}
Lungs	$4.2 \times 10^{-3} \pm 5.0 \times 10^{-4}$	1.8×10^{-5}	5.5×10^{-3}	8.1×10^{-4}	1.1×10^{-2}
Pancreas	$1.1 \times 10^{-2} \pm 1.4 \times 10^{-3}$	9.6×10^{-5}	6.8×10^{-3}	2.3×10^{-3}	2.0×10^{-2}
Red marrow	6.7×10^{-3}	1.9×10^{-4}	4.3×10^{-3}	1.0×10^{-3}	1.2×10^{-2}
Spleen	$1.4 \times 10^{-2} \pm 1.6 \times 10^{-3}$	8.4×10^{-5}	7.0×10^{-3}	1.4×10^{-3}	2.2×10^{-2}
Testes	4.4×10^{-3}	1.9×10^{-3}	9.1×10^{-3}	4.6×10^{-5}	1.5×10^{-2}
Thyroid		3.5×10^{-6}	1.2×10^{-2}	8.6×10^{-4}	1.3×10^{-2}
Uterus		5.5×10^{-3}	1.4×10^{-2}	2.2×10^{-4}	1.9×10^{-2}
Other tissue		5.2×10^{-6}	9.3×10^{-3}	7.5×10^{-4}	1.0×10^{-2}
				EDE: 2.4×10^{-2}	
					mSv/MBq

* Mean ± s.d.
† For 2-hr void time.
‡ For 1-hr void time.

TABLE 7
Absorbed Doses Reported by Various Authors Due to the Intravenous Administration of [^{18}F]FDG

Organs	Absorbed dose per unit of administered activity (mGy/MBq) Brownell et al. (1980)	Reivich et al. (1979)	Jones et al. (1982)	ICRP (1987)	This work	(1)§
Kidneys	1.4×10^{-2}	2.1×10^{-2}	1.9×10^{-2}	2.1×10^{-2}	‡ 3.0×10^{-2}	2.6×10^{-2}
Lungs	2.1×10^{-2}	1.8×10^{-2}	1.6×10^{-2}	1.1×10^{-2}	‡ 1.0×10^{-2}	9.4×10^{-3}
Liver	2.2×10^{-2}	1.8×10^{-2}	1.6×10^{-2}	1.2×10^{-2}	‡ 2.3×10^{-2}	2.1×10^{-2}
Spleen	3.9×10^{-2}	5.0×10^{-2}	3.9×10^{-2}	1.2×10^{-2}	‡ 2.2×10^{-2}	2.0×10^{-2}
Red marrow			1.1×10^{-2}	1.1×10^{-2}	1.2×10^{-2}	1.1×10^{-2}
Testes			1.5×10^{-2}	1.5×10^{-2}	1.5×10^{-2}	1.3×10^{-2}
Bladder wall	3.9×10^{-2}	7.8×10^{-2}	†‡ 1.1×10^{-1}	1.7×10^{-1}	†‡ 1.2×10^{-1}	9.1×10^{-2}
			†‡ 5.9×10^{-2}		†‡ 6.6×10^{-2}	
Brain	1.8×10^{-2}	1.8×10^{-2}	† 2.2×10^{-2}	2.6×10^{-2}	‡ 2.9×10^{-2}	2.8×10^{-2}
Heart	8.9×10^{-2}	4.0×10^{-2}	4.3×10^{-2}	6.5×10^{-2}	‡ 4.5×10^{-2}	4.3×10^{-2}
Pancreas	1.4×10^{-2}			1.2×10^{-2}	‡ 2.0×10^{-2}	1.8×10^{-2}

* For 2-hr void time.
† For 1-hr void time.
‡ Estimated from measurements in humans.
§ Absorbed doses calculated by using the "S" values for the American and European adult reference man.

to half of that for the 2-hr void time if the subjects void at 1 hr after injection. Mean absorbed dose to the brain was higher than that estimated by Jones, but this difference could be due to variations in the percentage of uptake in the human brain, which is dependent in normal subjects upon blood glucose levels and diet (*8*). We have observed the dependence of brain uptake with blood glucose concentration in various normal subjects undergoing brain glucose metabolism studies with FDG, and the relationship was adequately represented ($r = 0.998$) by a linear inverse regression ($p < 0.01$), suggesting that uptake in the brain increases at a low blood glucose level. Another factor for this difference is the relative weight of the brain to the total body, which can affect the organ biodistribution of this compound. A value of 2.6% is reported in Japanese adults (*19*), which is higher than the value (2%) for European and American adults (*20*). Absorbed doses evaluated from animal biodistribution data for the kidney and liver are 30% lower than the results obtained in this work, while lung and spleen estimates are 46% and 50% higher, respectively.

Absorbed doses calculated for European and American adults are lower than the results obtained for Japanese adults because the "S" values for the European and American adult reference man are lower than the corresponding values for Japanese (Table 7). Thus, an underestimation of the absorbed doses and the EDE to the Japanese would occur if the absorbed doses calculated for European and American adults are applied to Japanese adults.

The EDE due to the intravenous administration of FDG was estimated to be 2.4×10^{-2} mSv/MBq. The ICRP (Publication 53) reported a value of 2.7×10^{-2} mSv/MBq for European and American adults that is slightly higher than our result for Japanese adults. It is necessary to note that in the calculation of the absorbed dose to the bladder wall, the ICRP used the kidney-bladder model (*21*) and assumed a void period of 3.5 hr, which obviously results in a high dose to this organ.

In conclusion, we calculated the absorbed dose estimates in humans from biokinetic data obtained in man for most of the source organs after injection of [^{18}F]FDG. Although, the absorbed doses estimated in this work cannot be directly compared to other published data since there is organ weight/total body weight variance in Japanese versus European and American adults, the values reported here are in the range of other published results on the dosimetry of this radiopharmaceutical.

APPENDIX

Retention Functions and Equations Used in the Calculation of Cumulated Activities in Source Organs

For the liver, lung, kidney, pancreas, and spleen, the time-activity data were fitted to the function of two exponential terms from $t = 0$ to t' as:

$$A(t) = C_1 e^{-k_1 t} + C_2 e^{-k_2 t}, \qquad \text{Eq. A1}$$

where C_1, C_2 are the intercepts and k_1, k_2 are the biologic elimination constants. After $t = t'$, only physical decay was assumed, and the cumulated activity was obtained as:

$$\tilde{A} = \int_0^\infty A(t)dt = \frac{C_1}{(\lambda + k_1)} + \frac{C_2}{(\lambda + k_2)} (1 - e^{-(\lambda + k_2)\cdot t'}) + C_3 T_{phy} e^{-(\lambda \cdot t')}, \qquad \text{Eq. A2}$$

where λ and T_{phy} are the decay constant and the physical half-life of ^{18}F and C_3 is the last activity measured at time t' (last measurement time).

For the brain and heart, time-activity curves were expressed as a sum of five exponential terms

$$A(t) = \sum_{i=1}^{5} C_i(t) e^{-k_i \cdot t}, \qquad \text{Eq. A3}$$

where k_i is the kinetic rate constant determined from the three-compartment model for FDG. The cumulated activity can be obtained by integrating Equation A3 from zero to infinite time:

$$\tilde{A} = \sum_{i}^{5} \frac{C_i}{\lambda + k_i}. \qquad \text{Eq. A4}$$

Formulation Used to Calculate the "S" Values

For the brain, heart, and red marrow, the "S" values were calculated from the corresponding absorbed fractions, ϕ_i (*21*), organ weights, m (*11*), and equilibrium dose constants, Δ_i (*22*), as follows:

$$S = \frac{1}{m} \cdot \sum_{i} \phi_i \Delta_i. \qquad \text{Eq. A5}$$

For the remainder of the body, the "S" values were computed as recommended by Coffey and Watson (*23*) by the following equation:

$$S(r_k \leftarrow rb) = S(r_k \leftarrow tb) \frac{m_{tb}}{m_{rb}} - \sum_{h} S(r_k \leftarrow r_h) \frac{m_h}{m_{rb}}. \qquad \text{Eq. A6}$$

ACKNOWLEDGMENTS

The authors thank Dr. Hiroshi Yamaguchi of the National Institute of Radiological Sciences for providing the MIRD Tables for the Japanese physique; Dr. Satoshi Iwai for his helpful assistance and suggestions in this work; and to Mr. Shinya Seo for technical assistance.

REFERENCES

1. ICRP Publication 52. *Protection of the patient in nuclear medicine.* Oxford: Pergamon Press; 1987.
2. Snyder WS, Ford MR, Warner GG, Watson SB. "S" absorbed dose per unit cumulated activity for selected radionuclides and organs. *MIRD pamphlet no. 11.* New York: Society of Nuclear Medicine; 1975.
3. ICRP Publication 53. *Radiation dose to patients from radiopharmaceuticals.* Oxford: Pergamon Press; 1988.
4. Brownell GL, Ackerman RH, Strauss WH, et al. Preliminary imaging results with ^{18}F-2-fluoro-2-deoxy-D-glucose. *J Comput Assist Tomogr* 1980;4:473–477.
5. Reivich M, Kuhl D, Wolf A, et al. F-18-fluorodeoxyglucose method for the measurement of local cerebral glucose utilization in man. *Circ Res* 1979;44:127–137.
6. Jones SC, Alvai A, Christman D, Montanez I, Wolf AP, Reivich M. The radiation dosimetry of 2-[^{18}F]fluoro-2-deoxy-D-glucose in man. *J Nucl Med* 1982;23:613–617.
7. Gallagher BM, Ansari A, Atkins H, et al. Radiopharmaceuticals XXVII. ^{18}F-labeled 2-deoxy-2-fluoro-D-glucose as a radiopharmaceutical for measuring regional myocardial glucose metabolism in vivo: tissue distribution

and imaging in animals. *J Nucl Med* 1977;18:990–996.
8. Phelps ME, Hoffman EJ, Selin C, et al. Investigation of [^{18}F]2-fluoro-2-deoxyglucose for the measure of myocardial glucose metabolism. *J Nucl Med* 1978;19:1311–1319.
9. Eichling JO, Higgins CS, Ter-Pogossian MM. Determination of radionuclide concentrations with positron CT scanning (PETT): concise communication. *J Nucl Med* 1977;18:845–847.
10. Yamaguchi H, Nishizawa K, Maruyama T, Chiba M, Fukuhisa K, Hashizume T. A computer program to calculate MIRD Tables for Japanese physiques. *Hoken Butsuri* 1983;18:43–48.
11. Tanaka G. Japanese reference man 1988-III. Masses of organs and tissues and other physical properties. *Nippon Act Radiol* 1988;48:509–513.
12. Hoffman EJ, Phelps ME. Positron emission tomography: principles and quantitation. In: Phelps ME, Mazziota JC, Schelbert HR, eds. *Positron emission tomography and autoradiography: principles and applications for the brain and heart.* New York: Raven Press; 1986:237–286.
13. Smith EM. Calculating absorbed doses from radiopharmaceuticals. *Nucleonics* 1966;24:33–39.
14. Sokoloff L, Reivich M, Kennedy C, et al. The [^{14}C]deoxyglucose method for the measurement of local cerebral glucose utilization: theory, procedure, and normal values in the conscious and anesthetized albino rat. *J Neurochem* 1977;28:897–916.
15. Phelps ME, Huang SC, Hoffman EJ, Selin C, Sokoloff L, Kuhl DE. Tomographic measurement of local cerebral glucose metabolism rate in humans with [^{18}F]2-fluoro-2-deoxy-D-glucose: validation of method. *Ann Neurol* 1979;6:371–388.
16. Nakagawa T, Onayagi Y. Program system for statistical analysis with least squares fitting, SALS (version 2). User's manual. Part 1. Basic Usage. Univ. of Tokyo Computer Center, Tokyo. 1979.
17. ICRP Publication 26. *Recommendations of the international commission on radiological protection.* Oxford: Pergamon Press; 1977.
18. Woosley RL, Kim YS, Huang KC. Renal tubular transport of 2-deoxy-D-glucose in dogs and rats. *J Pharmacol Exp Ther* 1970;173:13–20.
19. ICRP Publication 23. *Report of task group on reference man.* Oxford: Pergamon Press; 1975.
20. Tanaka G, Kawamura H. Reference Japanese man-I. Mass of organs and other characteristics of normal Japanese. *Health Phys* 1979;36:333–346.
21. Snyder WS, Ford MR. Estimation of doses to the urinary bladder and to the gonads. In: *Radiopharmaceutical dosimetry symposium.* Rockville, MD: HEW Publication; 1976:313–349.
22. Cristy M, Eckerman KF. Specific absorbed fractions of energy at various ages from internal photon sources. VII. Adult male. Oak Ridge, TN: Oak Ridge National Laboratory; ORNL/TM-8381/V7; 1987.
23. Dillman LT, Von der Lage FC. Radionuclide decay schemes and nuclear parameters for use in radiation dose estimation. *MIRD Pamphlet 10.* New York: Society of Nuclear Medicine; 1975.
24. Coffey JL, Watson EE. Calculating dose from remaining body activity: a comparison of two methods. *Med Phys* 1979;6:307–308.